JOURNAL OF Materials CHEMISTRY

Incorporation and characterisation of oxides of manganese, cobalt and lithium into Nafion 117 membranes

Mikael Ludvigsson, Jan Lindgren* and Jörgen Tegenfeldt

Uppsala University, The Ångström Laboratory, Inorganic Chemistry, Box 538, SE-751 21 Uppsala, Sweden. E-mail: Jan.Lindgren@kemi.uu.se

Received 24th July 2000, Accepted 8th January 2001
First published as an Advance Article on the web 15th February 2001

Metal ion loaded Nafion membranes were used as starting materials in an *in situ* oxidation and precipitation process within the polymer membrane. The products achieved *via* this synthesis route were different amorphous and crystalline metal oxides like $LiCoO_2$ and Mn_3O_4 incorporated in the membrane either as a thin layer (skin) or throughout the whole membrane *via* a two way diffusion process. X-Ray diffraction and Raman spectroscopy were used for the characterisation of the incorporated species and the Nafion membrane. Crystalline phases could be identified using X-ray diffraction and Raman measurements were used to identify the amorphous precipitates.

1 Introduction

Many modern/potential future energy devices such as the Polymer Electrolyte Fuel Cell (PEFC), the Lithium Polymer Battery (LPB), smart windows and solar cells and also catalysts often include a thin film polymer as the electrolyte. In addition, different types of metal oxides can be used in all of the above applications either as intercalation hosts or as catalysing species.

Incorporation of the metal oxides into a polymer could increase the performance, *e.g.* by allowing more flexible mechanical handling and by creating a very intimate contact between electrolyte and metal oxide. The perfluorosulfonic ionomer Nafion from DuPont is well suited for applications such as this due to its microstructure of 40 Å inverted micelles that can take up water and in which the sulfonate groups (terminating the long pendant ether sidechains of the polymer) can act as ion-exchange sites.[1,2] Several studies of oxides incorporated into the Nafion membrane have been made over the last fifteen years, for example, Fe-oxide,[3-8] Pb-oxide,[9] Ru-oxide,[10–12] Ti-oxide,[8,13–18] U-oxide[12] and W-oxide.[19] Many different oxides have thus been incorporated into Nafion, but so far none of the layered cathode materials used in state of the art rechargeable lithium ion and lithium polymer batteries have been tried.

The anode of such batteries is usually made from graphite or coke where lithium ions can be intercalated and the cathode is made from lithium insertion compounds like $LiMn_2O_4$ and $LiCoO_2$.[20] Normally these two components are produced separately and then combined with the electrolyte to form the battery system. We thought that it should be possible to improve the final product by incorporating at least the transition metal oxide based cathode in the polymer membrane and thus create a very intimate contact at the molecular level between the electrolyte and the cathode. This could constitute the first step towards an all polymer battery. Clearly, in an actual battery cell or fuel cell the electrodes must also be electronic conductors. This could be accomplished, for example, by preconditioning the polymer membrane by including carbon black in a surface layer of the film, before incorporation of the appropriate metal oxide. Furthermore, in a *battery* application water cannot be tolerated in the membrane and must be replaced by a suitable organic solvent.

The incorporation of manganese oxide into a Nafion membrane has been achieved in two earlier studies, in both cases reporting an amorphous manganese oxide that could not be identified or characterised more fully.[21,22] In these composite materials the oxide particles are separated by the polymer matrix and hence the accessible surface area of the oxide is increased compared to bulk oxides. Since Nafion is well characterised and has good thermal and chemical stability we decided to use this polymer as a model system.

In our study, the aim was to incorporate oxides into the polymer membrane Nafion. Since cobalt and manganese are introduced in the membrane by ion exchange with a divalent cobalt or manganese salt, incorporation of $LiCoO_2$ or $LiMn_2O_4$ also requires an oxidation step. Depending on the method of oxidation, a series of different Co- and Mn-compounds can be formed besides $LiCoO_2$ and $LiMn_2O_4$, and in the present study we also investigate the conditions for formation of the various oxides.

Amorphous and crystalline particles were incorporated close to the surface within the membrane. X-Ray diffraction and Raman spectroscopy were used for the characterisation of the incorporated species and the Nafion membrane. Crystalline phases could be identified using X-ray diffraction. Raman measurements were used when identifying the phases of both amorphous and crystalline precipitates.

2 Experimental

The transparent 170 μm thick polymer Nafion 117 (DuPont) was boiled for 1 h in 10% H_2O_2, H_2O, 0.2 M H_2SO_4 and finally H_2O again to clean it and load it with hydrogen so that the Nafion–H form of the membrane was achieved. The Nafion–H membrane was cut into 2×2 cm pieces, a suitable size for the techniques used in this investigation. The membrane pieces were then ion-exchanged either in a 0.2 M MCl_2 or in a mixed 0.2 M MCl_2–0.2 M LiCl solution (where M is Mn or Co) for at least 24 hours prior to oxidation and precipitation. These ion exchange processes yielded metal ion loaded membranes, Nafion–M or Nafion–Li–M. Before the oxidation step each metal ion loaded Nafion membrane was thoroughly washed with deionized water to make certain that all metal ions corresponded stoichiometrically to the polymer sulfonate groups and that they were not solubilised in the water present

Table 1 Synthetic routes for incorporation of manganese containing precipitates into Nafion 117 membranes

Method	Starting material	Base	Oxidising agent	Temperature	Time	Precipitate
1A	Nafion–Mn	0.5 M NaOH (1 h)	0.2 M $K_2S_2O_8$ added (1 h)	25 °C	2 h	Black MnO_2 Mn_3O_4
1B	Nafion–Mn	0.5 M NaOH (0 h)	Oxygen gas bubbled (1 h)	25 °C	1 h	Black MnO_2 Mn_3O_4
1C	Nafion–Mn	2.5 M NaOH	Oxygen in solution	25 °C	24 h	Black MnO_2 Mn_3O_4
1D	Nafion–Mn	0.5 M NaOH (1 h)	0.2 M $K_2S_2O_8$ added (1 h)	70 °C	2 h	Black MnO_2 Mn_3O_4
1E	Nafion–H	0.5 M NaOH	Oxygen in solution	25 °C	24 h	Brown (OH) Black (Mn) Mn_3O_4 MnO_2
1F	Nafion–Li–Mn	0.5 M LiOH	Oxygen in solution	220 °C	24 h	Brown Mn_3O_4
1G	Nafion–Li–Mn	0.5 M LiOH	Oxygen in solution	180 °C	110 days	Greyish brown $Li_xMn_2O_4$
1H	Nafion–Li–Mn	2.5 M LiOH	Oxygen in solution	180 °C	7 days	Greyish brown $Li_xMn_2O_4$
1I	Nafion–Mn	2.5 M LiOH	Oxygen in solution	180 °C	7 days	Greyish brown
1J	Nafion–Mn_3O_4	2.5 M LiOH	—	180 °C	7 days	Greyish brown $Li_xMn_2O_4$

Table 2 Synthetic routes for incorporation of cobalt containing precipitates into Nafion 117 membranes

Method	Starting material	Base	Oxidizing agent	Temperature	Time	Precipitate (size)
2A	Nafion–Co	0.5 M NaOH	Oxygen in solution	25, 50, 100, 150, 200 °C	24 h	$HCoO_2$ Co_3O_4
2B	Nafion–Co	0.5 M NaOH	0.2 M $K_2S_2O_8$	70 °C	30 min	$HCoO_2$ (5 nm)
2C	Nafion–Li–Co	0.5 M LiOH	Oxygen in solution	180 °C	7 days	Co_3O_4 (8 nm)
2D	Nafion–Li–Co	2.5 M LiOH	Oxygen in solution	180 °C	7 days	$LiCoO_2$ (15 nm)
2E	Nafion–Co_3O_4 from 2C	2.5 M LiOH	Oxygen in solution	180 °C	7 days	Co_3O_4 $LiCoO_2$ (8 nm)
2F	Nafion–$HCoO_2$ from 2B	2.5 M LiOH	Oxygen in solution	180 °C	7 days	$LiCoO_2$ (10 nm)
2G	Nafion–$HCoO_2$ from 2A	2.5 M LiOH	Oxygen in solution	180 °C	7 days	$LiCoO_2$ (5–10 nm)

in the membrane. The metal oxide loaded membranes will also be referred to as for example Nafion–$LiCoO_2$.

Various methods for the oxidation of Mn and Co in the Nafion membranes are presented in Tables 1 and 2. The metal ion loaded membranes were treated differently with respect to temperature, time and alkaline concentration. These methods generally yielded a skin-like precipitation within the membrane.[3] In method 1E the hydrogen loaded membrane was used as a separator between two chambers filled with an Mn^{2+} solution and a NaOH solution, respectively. This prevents skin formation and a precipitate is obtained through the entire cross-section of the membrane. Experiments at 180 °C have been performed in a hydrothermal bomb with a Teflon interior.

Raman spectra were recorded at room temperature on a Renishaw 2000 micro Raman system equipped with a 25 mW 780 nm diode laser and a 20 mW 514 nm argon ion laser. Spectra were carefully recorded at low laser power to ensure that no phase transition would occur in the oxide and to prevent the polymer from being burnt. The influence of varying the laser power was monitored to see at what power the phase transitions started for the $\times 50$ microscope objective.

When examining the cross-section of a membrane it was first cut into two halves perpendicular to its surface. The membrane was placed between two microscope slides using double-sided tape. This assembly was polished on a rotating disc using the finest polishing paper with cooling water supplied.

The X-ray diffractograms were recorded on a Siemens D5000 diffractometer with Cu-Kα radiation. Profile analysis on the X-ray peaks was performed using the Scherrer formula.[23]

3 Results and discussion

3.1 The Nafion membrane

The Raman spectrum of a Nafion membrane contains a region between 700 and 400 cm^{-1} without any significant bands, Fig. 1, bottom spectrum. This is very fortunate in the study of transition metal oxide loaded membranes since their Raman active bands usually occur in this region. The strongest Nafion band at 730 cm^{-1} has been assigned earlier as a stretching mode of the CF_2 groups in the perfluorinated polymer backbone.[24] The X-ray diffractograms of the Nafion membrane contain two broad peaks at $2\theta = 17°$ and 40°, indicative of a totally amorphous polymer, Fig. 2, bottom diffractogram. The structure of the Nafion membrane itself has been thoroughly investigated in earlier work using techniques such as Mössbauer spectroscopy,[6,7] Fourier Transform Infrared (FTIR) spectroscopy[24–30] and Small Angle X-ray Scattering (SAXS).[1,31]

3.2 Raman laser power

In order to see how sensitive the samples were to laser heating, spectra of one of the samples (from method 1A, *cf.* Tables 1

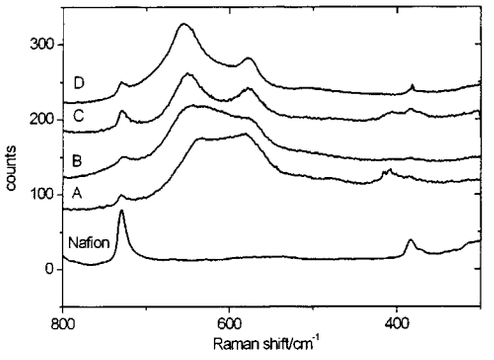

Fig. 1 From bottom to top: Raman spectra of an empty Nafion membrane and the manganese loaded membranes obtained from methods 1A, 1B, 1C and 1D.

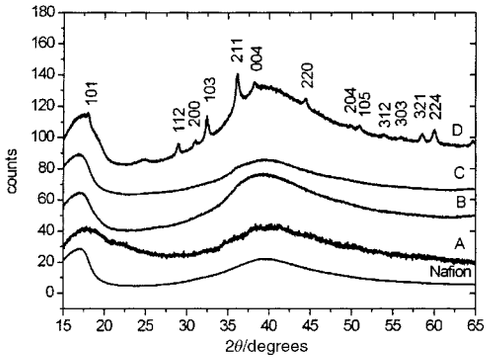

Fig. 2 From bottom to top: X-ray diffractogram of an empty Nafion membrane and the manganese loaded membranes obtained from methods 1A, 1B, 1C and 1D.

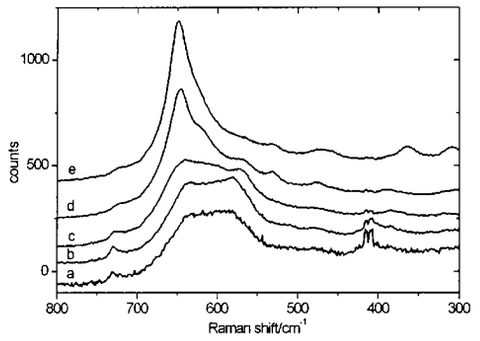

Fig. 3 Raman spectra where different laser powers are used, showing the phase transition of the manganese oxide in the membrane obtained from method 1A: (a) 0.05 mW, (b) 0.5 mW, (c) 1 mW, (d) 2 mW, (e) 4 mW.

and Fig. 3) were measured at different laser powers. In these measurements the influence of laser power on the membranes was investigated with the 25 mW red diode laser and the $\times 50$ objective. The 25 mW laser is reduced to ~ 5 mW when the power is measured at the sample. In addition, the power of the laser could be decreased to 1%–50% of this value, *i.e.* 0.05–2.5 mW. At low laser power where the laser signal is reduced to 1% (0.05 mW) and 10% (0.5 mW) at the sample the bands are located at 636 cm^{-1} and 578 cm^{-1} and at higher power the band at 636 cm^{-1} is shifted to higher wavenumbers. The results, shown in Fig. 3, indicates that a phase transition or some ordering/disordering in the sample occurs under the laser. It has been stated earlier that fine powders in particular are sensitive to treatments like this. This is consistent with the observed sensitivity of the fine particle precipitation in our membrane.[32]

3.3 Crystallite sizes

The crystallite sizes of the Mn_3O_4 formed in methods 1D and 1F could be estimated using both the X-ray diffractograms and the Raman spectra. The use of the Raman spectra for this purpose is based on a recent study investigating how the position and broadening of the Mn_3O_4 Raman band at ~ 650 cm^{-1} can give a size estimate for the crystallites in an Mn_3O_4 sample.[33] The authors of that study observed that the typical bulk Mn_3O_4 band at 660 cm^{-1} is broadened and shifted to lower wavenumbers as the crystallites become smaller. For crystallite sizes ranging from >50 to 20 nm the band position was found to change from 660 to 620 cm^{-1}. According to the authors,[33] the underlying reason for this behaviour is outlined in the Phonon confinement model: In an ideal infinite crystal, only phonons with $q \sim 0$, *i.e.* near the centre of the Brillouin zone, contribute to the Raman spectrum due to the momentum conservation between phonons and incident light, and hence the Raman peaks in a crystalline sample are sharp. However, for real and finite crystals, *e.g.* nanoparticles, defects and crystal boundaries will confine phonons in space. The result is an uncertainty in the phonon momentum, and phonons with $q \neq 0$ can contribute to the Raman spectrum, *i.e.* the Raman bands are broadened and shifted, as the particles become smaller. This effect is larger for smaller grain sizes.[33] The X-ray peaks in our study were analysed with normal profile analysis using the Scherrer formula. If the X-ray diffractograms are studied more in depth it can be seen that the two amorphous features in the pure Nafion diffractogram change when the membrane is loaded with an oxide. This is probably caused by broad peaks from the small particle phases of the oxides precipitated within the membrane since it seems unlikely that the oxides would induce alterations in the polymer itself.

3.4 Manganese loaded membranes

3.4.1 General. A large number of manganese oxide phases exist, some of which also occur as minerals. Some examples are: β-MnO_2 (pyrolusite, a tetragonal rutile structure where MnO_6 octahedra share two edges), α-MnO_2 (ramsdellite, an orthorhombic structure where MnO_6 octahedra share two edges), γ-MnO_2 (msutite, a mixture of ramsdellite and pyrolusite), Mn_2O_3 (bixbyite, cubic), α-MnOOH (groutite, orthorhombic), γ-MnOOH (manganite, monoclinic), Mn_3O_4 (hausmannite, distorted spinel).

Investigations of manganese oxide phases using Raman spectroscopy are numerous.[32,34–36] The analysis of the valency of the manganese ion is, however, very complex and the interpretation of the Raman spectra is not easy. In addition, many of the oxides undergo a phase transition when irradiated even by quite a low laser power. Therefore, care must be taken to avoid these phase transitions by using a low laser power, *ca.* 0.4–0.5 mW at the sample through a $\times 50$ microscope objective.

In earlier Raman studies of manganese oxides a 514 nm argon ion laser has usually been employed as the excitation source. However, using this type of laser produced a very poor Raman spectrum for the oxide/polymer systems in the present study and instead a 780 nm diode laser was chosen with excellent results.

In Fig. 1 the low laser power Raman spectra of samples obtained by methods 1A–1D are shown together with the pure Nafion–H membrane. Diffractograms of these samples are shown in Fig. 2.

The phases in samples obtained by methods 1A–1D are not easily identified. The diffractograms of samples obtained by methods 1A, 1B and 1C in Fig. 2 contain no sharp diffraction peaks but only the two broad and slightly modified features of the non-loaded membrane. All membranes are opaque and black so some material must be incorporated in all membranes. We also note that the high θ region in the diffractograms is broader relative to the low θ region than is the case for the empty membrane. However, the absence of sharp diffraction peaks implies that the incorporated material is amorphous or that the particles are very small. Attempts to subtract the X-ray diffractogram of an empty Nafion membrane from the loaded membranes were unsuccessful. In samples prepared by method 1D sharp diffraction peaks appear making it possible to identify that crystalline phase by diffraction whereas for samples obtained by methods 1A, 1B and 1C Raman spectroscopy is of more help.

3.4.2 MnO_2 and Mn_3O_4. In an extensive study Bernard *et al.*[32,35] found that the mineral hausmannite has a distinct feature at 651 cm^{-1} (s = strong) and two minor features at 365 and 315 cm^{-1}. In MnO_2 (ramsdellite and pyrolusite) samples they attributed bands at 650 (s), 576 (s) and 523 cm^{-1} (s) to typical vibrational modes for stoichiometric MnO_2. Another study reports that synthetic MnO_2, International Common Sample (ICS) no. 12, has Raman features at 410, 480, 520, 580, 640 cm^{-1}.[36] In that study the 580 cm^{-1} band was assigned to an Mn–O stretching vibration. The band at 578 cm^{-1} observed in the present study is thus typical for Mn(IV) oxides.

For methods 1A–1C there are no sharp diffraction peaks in contrast to the sharp diffraction peaks of the brown/black precipitate in method 1D making the latter diffractogram considerably more informative (Fig. 2). The data from method 1D can be successfully matched to the diffraction peaks of the Mn_3O_4 mineral hausmannite, which has a distorted spinel structure with tetragonal symmetry, space group $I4_1$.[37] A profile analysis using the Scherrer formula on the crystalline peaks in method 1D results in a size estimate for the incorporated Mn_3O_4 particles of ~ 15–20 nm.

The Raman spectra of the samples from methods 1C and 1D

are shown in Fig. 1. There are two distinct features at 655 and 577 cm^{-1}. The band at 655 cm^{-1} is typical for Mn_3O_4 and the band at 577 cm^{-1} is typical for MnO_2.[32,34,36,38] The band at 577 cm^{-1} vanishes for sufficiently large laser power and only the 655 cm^{-1} band is left.

From the above results we conclude that samples 1C and 1D consist of both Mn_3O_4 and MnO_2. We also conclude that at least part of the Mn_3O_4 is crystalline, whereas MnO_2 and possibly part of the Mn_3O_4 is either amorphous or consists of very small particles.

The position of the Raman band at 655 cm^{-1} suggests[33] crystallite sizes of $\sim$40 nm, somewhat larger than the estimate from the X-ray data but still of the same order of magnitude.

In method 1E, the membrane was used as a separator between two chambers filled with 0.2 M $MnCl_2$ and 0.5 M NaOH, respectively, for 24 hours. This asymmetric environment resulted in a precipitation throughout the membrane with different phases created on either side. On the cation side the same room temperature MnO_2-like phase was formed as above but interestingly enough, on the OH-side the crystalline hausmannite-like Mn_3O_4 phase/phase mixture appeared.

In an attempt to produce lithium containing oxides, the Nafion–Li–Mn membranes were kept in a hydrothermal bomb at an elevated temperature, 220 °C, for 24 hours (method 1F). In the process an Mn_3O_4 phase was formed instead, giving the same X-ray diffraction peaks as the mineral hausmannite described above, see Fig. 4.[37] A profile analysis of the diffraction peaks using the Scherrer formula yields oxide crystallite sizes around 25–30 nm in this membrane. There are two peaks at $2\theta = 18.5°$ and $2\theta = 55°$ that can not be accounted for by Mn_3O_4 or by lithium manganese oxides. The peaks do not correspond to major peaks in any other manganese oxide. The Raman spectra in Fig. 5 confirm the presence of the Mn_3O_4 phase with one major band at 658 cm^{-1} and three minor bands at 370, 317 and 288 cm^{-1}.[2] The 288 cm^{-1} band has not been assigned previously to Mn_3O_4. However, since a 780 nm Raman spectrum of Mn_3O_4 has not been reported earlier it can not be ruled out that the band belongs to Mn_3O_4.

The spectra of the samples prepared by this hydrothermal process were of very good quality. This encouraged us to perform a phase analysis across the cross-section of the membrane using Raman spectroscopy. The membrane was cut into two halves and the cross-section was polished for the Raman measurements, see Fig. 6. Only one half of the membrane was examined since the membrane had been treated symmetrically during all steps in the synthesis. The spectra obtained from a cross-section of the membrane are displayed in Fig. 5.

Using the relative band intensities of the Mn_3O_4 band at 658 cm^{-1} and the major Nafion band at 730 cm^{-1} it is possible to plot the oxide concentration profile across the membrane, Fig. 7. The spectra indicate that the Mn_3O_4 surface phase is present also within the membranes but the concentration of oxide decreases inside the membrane. This observation corresponds well with the skin-like behaviour seen in earlier incorporations of metal oxides into Nafion membranes.[3] The crystallite sizes can be estimated to be $\sim$45 nm using the Raman band position as discussed above.[33] This value is somewhat larger than the one determined by X-ray diffraction but of the same order.

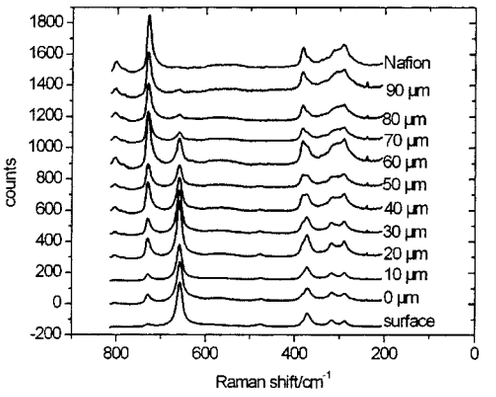

Fig. 5 The Raman spectra of the cross-section of the manganese loaded membrane obtained in method 1F. The bottom spectrum is from the surface of the membrane and the 0, 10, 20, 30… μm curves are cross-section spectra at these depths. The top spectrum shows an empty Nafion membrane.

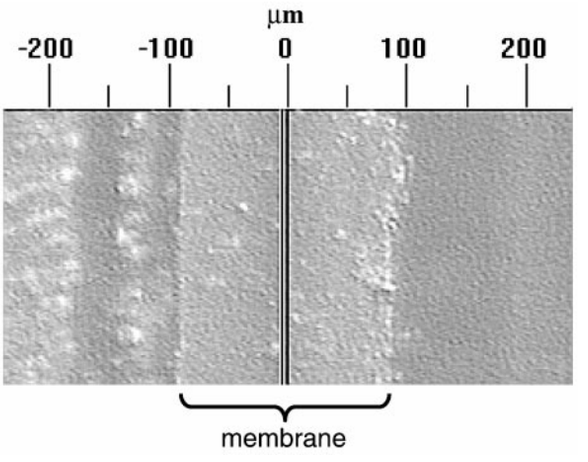

Fig. 6 Picture of the cross-section of the method 1F manganese loaded membrane.

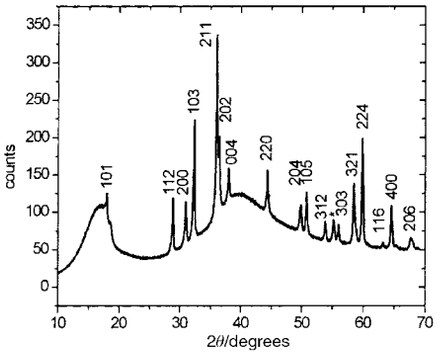

Fig. 4 X-Ray diffractogram of the manganese loaded membrane obtained in method 1F. The peaks are assigned as belonging to an Mn_3O_4 phase.

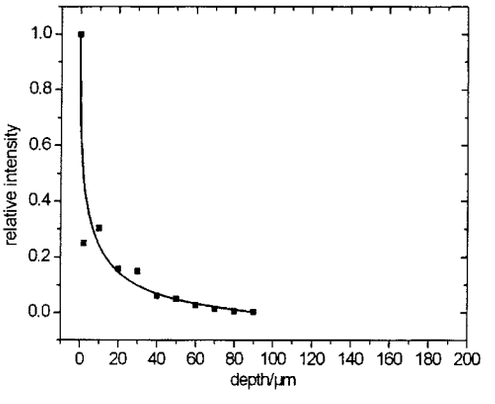

Fig. 7 The oxide profile in the method 1F manganese loaded membrane. The values are obtained from the relative intensities of the 730 cm^{-1} band of Nafion and the 658 cm^{-1} band of the oxide.

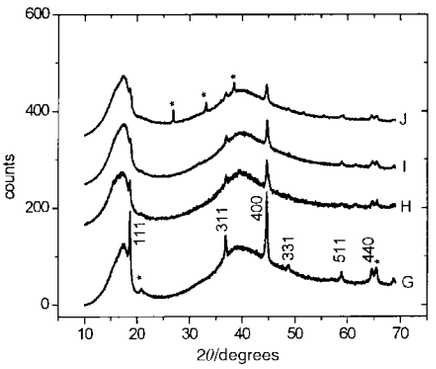

Fig. 8 X-Ray diffractograms of the manganese loaded membranes obtained in methods 1G, 1H, 1I and 1J. The same $Li_xMn_2O_4$ peaks are found in all diffractograms. Peaks of unknown origin are marked (*).

3.4.3 $Li_xMn_2O_4$. Previously reported incorporations of metal oxides in Nafion membranes, as mentioned in the introduction, suggested to us that it might be possible to incorporate lithium manganese oxides within an ionomeric membrane. One suitable candidate is the spinel $LiMn_2O_4$ that is used as cathode material in state of the art lithium polymer batteries and lithium ion batteries. In our attempts to incorporate a lithium manganese oxide the preparation methods 1G–1J (see Table 1) were explored. For all of these methods a lithiated phase was formed.

The X-ray diffractograms of the resulting membranes 1G to 1J, Fig. 8, show the typical peaks of a cubic spinel of space group *Fd3m*. The peaks are situated between those of a $LiMn_2O_4$ phase and a $Li_xMn_2O_4$ phase ($x\rightarrow0$).[39,40] This indicates that the present phase is probably $Li_xMn_2O_4$ ($0<x<1$) and not a pure λ-MnO_2 phase or $LiMn_2O_4$ phase. For method 1G there is a peak at $2\theta=20.7°$ and another one close to 66° that might be due to small amounts of Li_2MnO_3 as an impurity phase.[41] For method 1J, three unidentified peaks at $2\theta=26.9$, 33.1 and 38.5° are observed.

To investigate the membrane further, Raman spectroscopy was used since different amounts of lithium within the cubic MnO_2–$LiMn_2O_4$ structure yield different Raman spectra (Table 3).[42–44] There are five main features in the Raman spectrum at 616, 570, 497, 437 and 375 cm^{-1}, see Fig. 9. These bands have been observed in the lithium manganese oxide spinels in an earlier study.[42] Calculations and assignments of bands in that study show that $LiMn_2O_4$ has bands at 625, 480, 432, and 365 cm^{-1}, the isostructural λ-MnO_2 has bands at 647, 592, 498 and 463 cm^{-1} and finally the $Li_{0.5}Mn_2O_4$ phase has bands at 657, 630, 612, 597, 560, 493, and 296 cm^{-1}. These data together with our results are summarised in Table 1. Unfortunately, if the data in Table 1 is carefully examined it is clear that the spectrum of the method 1G precipitate is not a perfect fit to any one of the three phases. The band at 615 cm^{-1} indicates $Li_{0.5}Mn_2O_4$ but the bands at 430 and 370 cm^{-1} are typical for $LiMn_2O_4$ and the band at 493 cm^{-1} could belong to the λ-MnO_2 phase. Nevertheless, there are a number of features giving strong indications of a lithium manganese oxide phase in this sample: A band between 610 and 630 cm^{-1} seems to exist

Table 3 Raman shift (in cm^{-1}) and band assignments for different lithium manganese oxides[42]

$LiMn_2O_4$[42]	$Li_{0.5}Mn_2O_4$[42]	λ-MnO_2[42]	Symmetry[42]	Bands in methods 1G–1J
625	657, 597, 560	597	A_{1g}	616
590	630, 612	647	T_{2g}	570
480	493	498	T_{2g}	497
432	—	463	E_g	437
365	296	—	T_{2g}	375

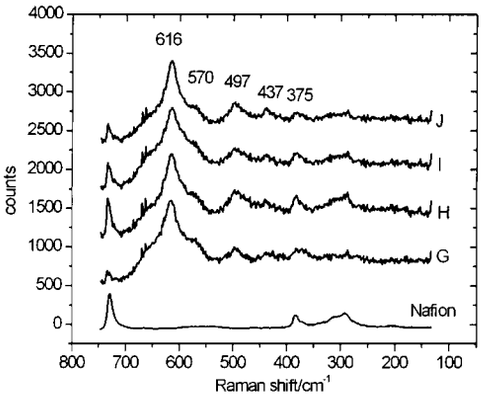

Fig. 9 The Raman spectra of the manganese loaded membranes in methods 1G, 1H, 1I and 1J are similar with features at 616, 570, 497, 437 and 375 cm^{-1}.

only in a lithiated sample, the bands at 437 and 375 cm^{-1} are only observed in $LiMn_2O_4$ and the band at 497 cm^{-1} is observed in $Li_{0.5}Mn_2O_4$ and shifted by 15 cm^{-1} in $LiMn_2O_4$.

Since the Mn_3O_4 phase incorporated in method 1F belongs to a structure that can be described as a distorted spinel structure we decided to attempt an ion exchange on this precipitate and thus achieve the desired lithiated spinel structure. A method 1F membrane was therefore placed in a 2.5 M LiOH solution in a hydrothermal bomb at 180 °C for 7 days (method 1J). The X-ray diffractogram before the ion exchange can be seen in Fig. 4 and after the ion exchange in Fig. 8. The two diffractograms are clearly different. The typical *Fd3m* peaks are well defined and in the same position as in method 1G, 1H and 1I. Also the Raman spectrum of this sample shows the same pattern as the previous lithiated oxides.

3.5 Cobalt loaded membranes

3.5.1 General. Several cobalt oxides exist and two of these were identified in this study, Co_3O_4 and $HCoO_2$. Co_3O_4 crystallises as a normal spinel structure $Co^{2+}Co^{3+}{}_2O^{2-}{}_4$ (space group *Fd3m*). The Co^{2+} ions are in isolated tetrahedral sites and the Co^{3+} ions are octahedrally coordinated where these octahedra are interlinked.[45,46]

The oxohydroxide of cobalt, $HCoO_2$ or CoOOH, is isostructural with the layered rhombohedral HT-$LiCoO_2$ compound described more extensively below. The mineral form of $HCoO_2$ is also known as heterogenite-3R.[47]

As summarised in Table 2, the various synthetic routes employed produced different cobalt compounds. The identification and characterisation of these are discussed below.

3.5.2 $HCoO_2$ and Co_3O_4. We expected that we could obtain different cobalt oxides during our efforts to achieve a lithium cobalt oxide within the Nafion membrane. Earlier studies of oxide incorporation in Nafion membranes have shown that different oxides are produced at different temperatures.[3] Therefore we performed a temperature study of incorporations within the membrane. Five Nafion–Co membranes were placed in a hydrothermal bomb filled with a 0.5 M NaOH solution for 24 hours at 25, 50, 100, 150 and 200 °C. NaOH solution was used to ensure that there were no lithiated phases in these precipitations, and oxidation was accomplished utilising the oxygen present in the solution. The X-ray diffractograms of these reference precipitations are shown in Fig. 10. According to the X-ray diffractograms the incorporated species were $HCoO_2$ for the sample prepared at 25 °C (Nafion–$HCoO_2$ from method 2A) and Co_3O_4 at 200 °C (Nafion–Co_3O_4 from 2A) and mixtures between these two for intermediate temperatures. The broad low and high θ features belong to the amorphous polymer fraction.

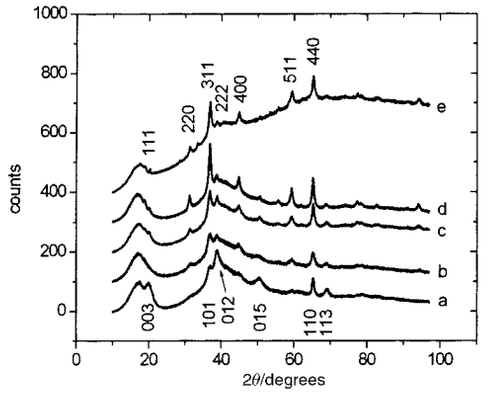

Fig. 10 X-Ray diffractograms of Nafion membranes loaded with cobalt oxides. The Nafion–Co membranes were placed in hydrothermal bombs filled with 0.5 M NaOH at 25 °C (a), 50 °C (b), 100 °C (c), 150 °C (d) and 200 °C (e).

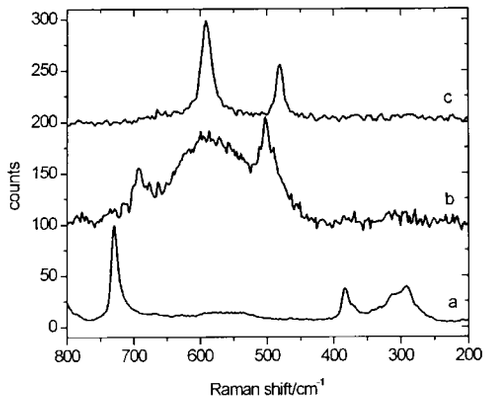

Fig. 11 Raman spectra of an empty Nafion membrane (a), the $HCoO_2$ loaded membrane (b) from method 2B and the same membrane but now $LiCoO_2$ loaded in method 2F (c).

The Nafion–$HCoO_2$ sample from 2B was found to be very sensitive to laser heating when the Raman spectra were recorded and low laser power had to be used to avoid phase transitions. At high laser power the oxide in the Nafion–$HCoO_2$ sample from 2B was reduced to Co_3O_4. At the lowest power ($\sim$0.1 mW at the membrane) there are three main features in the spectrum: a band at 693 cm^{-1}, a broad band centred at 585 cm^{-1} and a strong band at 501 cm^{-1}, Fig. 11. When the laser power is increased the features at 585 and 501 cm^{-1} vanish, the band at 693 cm^{-1} gets stronger and new bands appear at 520 and 476 cm^{-1}. It is worth noting that the intensity of the band at $\sim$693 cm^{-1} is increased and the position is shifted to 685 cm^{-1} at 0.5 mW. This behaviour is observed also for the Co_3O_4 band at this position in Nafion–Co_3O_4 (from 2C) below. The features at 585 and 501 cm^{-1} in the 0.1 W spectrum are attributed to vibrational modes of $HCoO_2$. Due to the similarity between the $HCoO_2$ and the $LiCoO_2$ structures the two bands could be assigned as the A_{1g} (585 cm^{-1}) and the E_g (501 cm^{-1}) modes corresponding to the

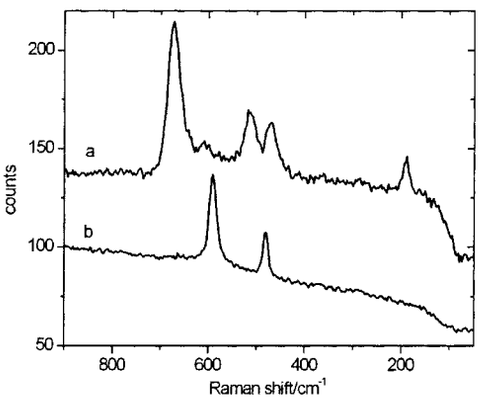

Fig. 12 Raman spectra of the Co_3O_4 loaded membrane in method 2C (a) and the $LiCoO_2$ loaded membrane in method 2D (b).

A_{1g} (595 cm^{-1}) and E_g (485 cm^{-1}) bands in $LiCoO_2$, see below. Further support for this assignment can be found in Raman spectra of the isostructural NiOOH structures that have bands at 560 and 480 cm^{-1} assigned as A_{1g} and E_g respectively.[48]

In method 2C an unsuccessful attempt was made to produce a lithiated oxide and the Raman spectrum of the precipitate verifies that the Co_3O_4 phase is present, Fig. 12. Among the vibrational modes of this spinel there are five Raman active modes: $A_{1g}+E_g+3F_{2g}$.[49] These five vibrations have been observed previously by different research groups.[50,51] The top spectrum in Fig. 12 is from the Nafion–Co_3O_4 (from 2C) membrane. Each band in this spectrum can be assigned to a Co_3O_4 vibrational mode, see Table 4.[50,51] It is interesting to note that the bands are shifted downwards at high laser power. The A_{1g} band at 691 cm^{-1} is shifted as much as 17 cm^{-1} for 5 mW at the membrane, Table 4.

3.5.3 $LiCoO_2$. The layered $LiCoO_2$ compound has the rhombohedral α-$NaFeO_2$ structure with face-sharing CoO_6 octahedra, space group *R3m*. The lithium and cobalt ions occupy alternating layers in the (111) direction, Co–O–Li–O–Co–O–Li–. The structure can also be viewed as edgesharing CoO_6 octahedra with lithium ions stacked in 3b sites between CoO_2-layers.[47,52] This phase is commonly known as the high temperature phase (HT-$LiCoO_2$).[53] In the same study a low temperature phase (LT-$LiCoO_2$) has also been reported. The authors found that the difference between the HT- and the LT-phase is found in the Co- and Li-layers. In the LT-$LiCoO_2$ structures 6% of the sites in the Li-layers are occupied by cobalt ions and 4% of the sites in the Co-layers are occupied by lithium ions. The difference between the two phases is reflected in a shorter *c*-axis in LT-$LiCoO_2$ (13.89 Å) than in HT-$LiCoO_2$ (14.05 Å).

$LiCoO_2$ has in total 6 vibrational modes of which 3 are degenerate: A_{1g}, E_g, $2A_{2u}$ and $2E_u$. The two first are Raman active and are located at 597 cm^{-1} (A_{1g}) and 485 cm^{-1} (E_g). The A_{2u} and E_u modes are IR-active.[54,55] The A_{1g} mode is a symmetric stretching mode of the CoO_6 octahedra and twice as strong as the E_g bending mode of O–C–O entities. In a Raman spectroscopy study of HT-$LiCoO_2$ and LT-$LiCoO_2$ it was

Table 4 Assignments and Raman shifts for incorporated Co_3O_4 and $LiCoO_2$ in this study and for Co_3O_4 and $LiCoO_2$ in earlier reports[49,54]

	Raman shift/cm^{-1}			
Vibrational mode[49]	Co_3O_4[49]	Co_3O_4 in Nafion, 0.1 mW (5 mW)	$LiCoO_2$[54]	$LiCoO_2$ in Nafion, 0.1 mW (5 mW)
A_{1g}	691	691 (674)	595	595 (588)
F_{2g}	618	(609)	—	—
F_{2g}	522	523 (513)	—	—
E_g	482	483 (471)	485	485 (477)
F_{2g}	194	(190)	—	—

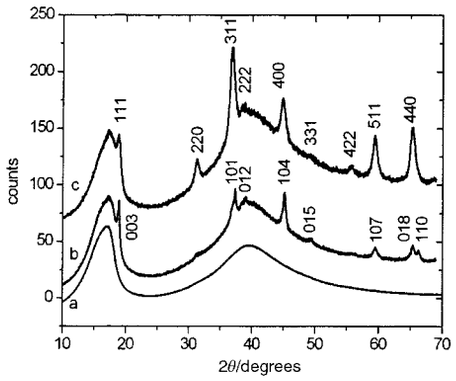

Fig. 13 X-Ray diffractograms of an empty Nafion membrane (a), the $LiCoO_2$ loaded membrane from method 2D (b) and the Co_3O_4 loaded membrane from method 2C (c).

found that the Raman spectrum of HT-$LiCoO_2$ contains two well defined bands at 596 and 487 cm^{-1} and a LT-$LiCoO_2$ spectrum contains three bands at 582, 475 and 447 cm^{-1}.[56] In another study Huang and Frech report two bands at 595 and 486 cm^{-1} for HT-$LiCoO_2$ and four bands at 603, 583, 478 and 445 cm^{-1} for the LT-$LiCoO_2$.[57] The HT- and the LT-structure can thus be easily distinguished with both X-ray diffraction and Raman spectroscopy.

The stronger 2.5 M LiOH solution used in method 2D gave another phase than the Nafion–Co_3O_4 obtained in method 2C. The X-ray diffractogram of the method 2D membrane can be indexed as the rhombohedral HT-$LiCoO_2$ phase with all $LiCoO_2$ peaks matching well, Fig. 13.[47,52,58]

The X-ray diffractograms of samples from methods 2C (Nafion–Co_3O_4) and 2D (Nafion–$LiCoO_2$) are almost identical but with some significant differences, compare diffractograms in Fig. 13. The diffractogram of Nafion–Co_3O_4 from 2C was successfully indexed as the Co_3O_4 spinel structure and that of Nafion–$LiCoO_2$ from 2D was indexed as the rhombohedral $LiCoO_2$ structure. Although the diffractograms of the two structures are similar they contain features that distinguish one from the other, *e.g.* the Co_3O_4 (220) peak and the $LiCoO_2$ (110) peak. Many of the other peaks are close but the (101) peak of Nafion–$LiCoO_2$ from 2D is well defined with only a small shoulder from the (311) peak of the Nafion–Co_3O_4 sample from 2C.

The Raman spectrum of the $LiCoO_2$ incorporated in method 2D consists of two bands at 485 and 595 cm^{-1} corresponding to the Raman active E_g and A_{1g} modes mentioned above, Fig. 12 and Table 4. No other bands are present in the spectrum indicating that there is no other phase in the membrane.

An *in situ* incorporation of $LiCoO_2$ was thus achieved in the membrane in method 2D. As was shown in method 2A, $HCoO_2$ is formed at room temperature, Co_3O_4 at elevated temperatures and a mixture of the two phases at intermediate temperatures. The process of incorporation in method 2D could thereby go *via* a cobalt oxide to the lithium cobalt oxide. An investigation whether this lithiation was possible for oxides already within the membrane was needed. This was performed for the Co_3O_4 phase from method 2C and the $HCoO_2$ phase from methods 2A and 2B. The isostructural $HCoO_2$ is the more probable candidate for lithiation since it has been shown earlier that a lithiation of this compound is possible.[47] To our knowledge no attempt has been made to use Co_3O_4 as starting material. This is a more complex process due to the difference in structures of Co_3O_4 and $LiCoO_2$.

Methods 2E to 2G explore the possibility of using Co_3O_4 and $HCoO_2$ as starting materials for lithiation. The success of the lithiation was verified using both X-ray diffraction and Raman spectroscopy as described above.

4 Conclusions

This study shows that it is possible to achieve manganese and cobalt oxide phases through an *in situ* precipitation of the oxide within a polymer membrane. This can be done in an aqueous solution at moderate temperatures, which is advantageous compared with many other techniques.

We have also shown that lithiated oxides can be obtained either in direct lithiation or using an ion exchange on the oxides Mn_3O_4, Co_3O_4 and $HCoO_2$ within a membrane.

For the manganese oxides it seems clear that the choice of oxidising agent does not influence the product as much as the temperature does since precipitations of different oxide phases are the same at each specific temperature irrespective of the oxidising agent used. At higher temperatures above 70 °C an in part crystalline hausmannite-like (Mn_3O_4) phase is created and at lower temperatures a more amorphous MnO_2-like phase probably consisting of nano sized particles is created. Similarly, for cobalt oxides the temperature has a strong influence on the final product, $HCoO_2$ being formed preferentially at low temperatures and Co_3O_4 at high temperatures.

Raman spectroscopy was a useful tool that could indicate the probable phase even when the Raman bands are quite broad because of the small particle size. We also found that Raman spectroscopy can be used as a phase sensitive tool when studying the cross-sections of the membranes in this study. This could be of great interest also in other applications where element specific analysis techniques have been used earlier.

The small particle precipitations within the Nafion membrane were just as in earlier studies observed to be sensitive to reduction due to laser heating. It is important to note that all precipitations involving Mn in this study are probably phase mixtures of at least two manganese oxide phases since the manganese oxide system is known to have a complex valency.

This study is intended as a first step in exploring the possibilities to incorporate electroactive materials in polymer membranes for possible use in devices like lithium polymer batteries, sensors and catalysers. A further characterisation using electrochemical methods is, however, required.

Acknowledgements

The Swedish Natural Science Research Council (NFR) has financially supported this work and this is hereby gratefully acknowledged.

References

1 T. D. Gierke, G. E. Munn and F. C. Wilson, *J. Polym. Sci., Polym. Phys. Ed.*, 1981, **19**, 1687.
2 H. L. Yeager and A. Steck, *J. Electrochem. Soc.*, 1981, **128**, 1880.
3 L. Raymond, J.-F. Revol, D. H. Ryan and R. H. Marchessault, *J. Appl. Polym. Sci.*, 1996, **59**, 1073.
4 K. Tennakone, O. A. Ileperuma, J. M. S. Bandara, C. T. K. Thaminimulla and U. S. Ketipearachchi, *J. Chem. Soc., Chem. Commun.*, 1991, 579.
5 M. Pineri, J. C. Jesior and J. M. D. Coey, *J. Membr. Sci.*, 1985, **24**, 325.
6 A. Meagher, B. Rodmacq, J. M. D. Coey and M. Pineri, *React. Polym.*, 1984, **2**, 51.
7 A. Meagher, B. Rodmacq, J. M. D. Coey and M. Pineri, *NATO ASI Ser., Ser. E*, 1985, 332.
8 H. Yoneyama, *Res. Chem. Intermed.*, 1991, **15**, 101.
9 Z. Ogumi, T. Mizoe, Z. Chen and Z.-I. Takehara, *Bull. Chem. Soc. Jpn.*, 1991, **64**, 1261.
10 A. Michas and P. Millet, *J. Membr. Sci.*, 1991, **61**, 157.
11 A. Michas, J. M. Kelly, R. Durand, M. Pineri and J. M. D. Coey, *J. Membr. Sci.*, 1986, **29**, 239.
12 A. Michas, R. Durand, J. C. Jesior, J. M. Kelly and M. Pineri, *Ann. Phys.*, 1986, **11**, 121.
13 M. Watanabe, H. Uchida and M. Emori, *J. Phys. Chem. B*, 1998, **102**, 3129.

14 A. Albu-Yaron, L. Arcan and C. Heitner-Wirguin, *Thin Solid Films*, 1990, **185**, 181.
15 F. F. Fan, H.-Y. Liu and A. J. Bard, *J. Phys. Chem.*, 1985, **89**, 4418.
16 E.-A. Lund, E. Blatt, D. N. Furlong, A. W.-H. Mau and W. H. F. Sasse, *Aust. J. Chem.*, 1989, **42**, 1367.
17 R. Dabestani, X. Wang, A. J. Bard, A. Campion, M. A. Fox, S. E. Webber and J. M. White, *J. Phys. Chem.*, 1986, **90**, 2729.
18 H. Miyoshi, S. Nippa, H. Uchida, H. Mori and H. Yoneyama, *Bull. Chem. Soc. Jpn.*, 1990, **63**, 3380.
19 F. Michalak, L. Rault and P. Aldebert, *SPIE*, 1992, **1728**, 278.
20 R. Koksbang, J. Baker, H. Shi and M. Y. Saidi, *Solid State Ionics*, 1996, **84**, 1.
21 Z. Ogumi, T. Mizoe, Z. Chen and Z.-I. Takehara, *Bull. Chem. Soc. Jpn.*, 1990, **63**, 3365.
22 Z. Chen, T. Mizoe, Z. Ogumi and Z.-I. Takehara, *Bull. Chem. Soc. Jpn.*, 1991, **64**, 537.
23 B. D. Cullity, *Elements of X-ray diffraction*, Addison-Wesley Publication Co., Reading, 1978.
24 J. Ostrowska and A. Narebska, *Colloid Polym. Sci.*, 1983, **261**, 93.
25 M. Falk, *Can. J. Chem.*, 1980, **58**, 1495.
26 C. Heitner-Wirguin, *Polymer*, 1979, **20**, 371.
27 D. Nandan, K. K. Pushpa, V. B. Kartha, P. K. Wahi and R. M. Iyer, *Indian J. Chem.*, 1994, **33A**, 395.
28 S. Quezado and J. C. T. Kwak, *Can. J. Chem.*, 1984, **62**, 958.
29 M. Ludvigsson, J. Lindgren and J. Tegenfeldt, *J. Electrochem. Soc.*, 2000, **147**, 1303.
30 M. Ludvigsson, J. Lindgren and J. Tegenfeldt, *Electrochim. Acta*, 2000, **45**, 2267.
31 R. B. Moore and C. B. Martin, *Macromolecules*, 1988, **21**, 1334.
32 M.-C. Bernard, A. Hugot-Le Goff, B. V. Thi and S. Cordoba de Torresi, *J. Electrochem. Soc.*, 1993, **140**, 3065.
33 J. Zuo, C. Xu, Y. Liu and Y. Qian, *Nanostruct. Mater.*, 1998, **10**, 1331.
34 B. A. Lopez de Mishima, T. Ohtsuka and N. Sato, *J. Electroanal. Chem.*, 1988, **243**, 219.
35 M.-C. Bernard, S. Cordoba de Tooresi, A. Hugot Le-Goff and B. Vu Thi, *Proc. Electrochem. Soc.*, 1994, **94**, 146.
36 B. A. Lopez de Mishima, T. Ohtsuka and N. Sato, *Electrochim. Acta*, 1993, **38**, 341.
37 D. Jarosch, *Miner. Petr.*, 1987, **37**, 15.
38 D. Gosztola and M. J. Weaver, *J. Electroanal. Chem.*, 1989, **271**, 141.
39 M. M. Thackeray, P. J. Johnson, L. A. De Picciotto, P. G. Bruce and J. B. Goodenough, *Mater. Res. Bull.*, 1984, **19**, 179.
40 A. Schmierr and G. Sterr, *Naturwissenschaften*, 1965, **52**, 392.
41 P. Strobel and B. Lambert-Andron, *J. Solid State Chem.*, 1988, **75**, 90.
42 B. Ammundsen, G. R. Burns, M. S. Islam, H. Kanoh and J. Roziere, *J. Phys. Chem.*, 1999, **103**, 5175.
43 W. Huang and R. Frech, *J. Power Sources*, 1999, **81–82**, 616.
44 H. Kanoh, W. Tang and K. Ooi, *Electrochem. Solid State Lett.*, 1998, **1**, 17.
45 W. L. Roth, *J. Phys. Chem. Solids*, 1964, **25**, 1.
46 X. Liu and C. T. Prewitt, *Phys. Chem. Miner.*, 1990, **17**, 168.
47 G. G. Amatucci, J. M. Tarascon, D. Larcher and L. C. Klein, *Solid State Ionics*, 1996, **84**, 169.
48 J. Desilvestro, D. A. Corrigan and M. J. Weaver, *J. Electrochem. Soc.*, 1988, **135**, 4.
49 D. L. Rousseau, R. P. Bauman and S. P. S. Porto, *J. Raman Spectrosc.*, 1981, **10**, 253.
50 H. Shirai, Y. Morioka and I. Nakagawa, *J. Phys. Soc. Jpn.*, 1982, **51**, 592.
51 V. G. Hadjiev, M. N. Iliev and I. V. Vergilov, *J. Phys C: Solid State Phys.*, 1988, **21**, L199.
52 G. G. Amatucci, J. M. Tarascon and L. C. Klein, *J. Electrochem. Soc.*, 1996, **143**, 1114.
53 R. J. Gummow, M. M. Thackeray, W. I. F. David and S. Hull, *Mater. Res. Bull.*, 1992, **27**, 327.
54 T. Itoh, H. Sato, T. Nishina, T. Matue and I. Uchida, *J. Power Sources*, 1997, **68**, 333.
55 C. Julien and G. A. Nazri, *Mater. Res. Soc. Symp. Proc.*, 1999, **548**, 79.
56 S. G. Kang, S. Y. Kang, K. S. Ryu and S. H. Chang, *Solid State Ionics*, 1999, **120**, 155.
57 W. Huang and R. Frech, *Solid State Ionics*, 1996, **86–88**, 395.
58 W. D. Johnston, R. R. Heikes and D. Sestrich, *Mater. Res. Bull.*, 1958, **7**, 1.